Article

Discovery Medicine 2026; 38(210): 2153–2163
https://doi.org/10.24976/Discov.Med.202638210.168

Chitosan Oligosaccharide Suppresses Fibronectin- and Osteopontin-Associated Malignant Phenotypes in A2058 Melanoma Cells

In Youb Chang[1], Young Hee Maeng[2], Hye-Jin Boo[3], Jin Won Hyun[3], Sang-Pil Yoon[3,4,*]

[1]Department of Anatomy, Chosun University School of Medicine, 61452 Gwangju, Republic of Korea
[2]Department of Pathology, College of Medicine, Jeju National University, 63243 Jeju, Republic of Korea
[3]Jeju Research Center for Natural Medicine, Jeju National University, 63243 Jeju, Republic of Korea
[4]Department of Anatomy, College of Medicine, Jeju National University, 63243 Jeju, Republic of Korea
*Correspondence: spyoon@jejunu.ac.kr (Sang-Pil Yoon)
Submitted: 5 March 2026 Revised: 20 May 2026 Accepted: 10 June 2026 Published: 23 July 2026

Background: While chitosan oligosaccharide (COS) has been reported to exert anti-tumor and immunomodulatory effects, its functional impact on malignant melanoma remains poorly defined. Herein, we investigated the biological actions of COS in A2058 human melanoma cells, focusing on malignant behavior.

Methods: COS was prepared from highly deacetylated, low-viscosity chitosan and applied to A2058 cells under conventional monolayer culture and spheroid formation cultures in fetal bovine serum (FBS)- or growth factor (GF)–supplemented conditions. Cell viability, migration, spheroid formation, Western blotting for epithelial-mesenchymal transition and aggressiveness were assessed. Immunohistochemistry was used to evaluate osteopontin expression in human skin cancer tissue microarrays.

Results: Although COS exhibited limited direct cytotoxicity in A2058 melanoma cells, it suppressed spheroid formation. Fibronectin, upregulated during spheroid formation, was reversed by COS in a concentration-dependent manner, whereas other epithelial-mesenchymal markers were less consistently affected. COS significantly downregulated osteopontin in monolayer and spheroids in GF-supplemented conditions. While exogenous recombinant osteopontin enhanced migration in a dose-dependent manner, low-dose COS (50 µg/mL) abolished this pro-migratory effect. In tissue microarrays, osteopontin immunostaining was higher in normal skin than in melanoma and tended to decrease with stage advancement. While COS did not alter the secretory fraction of osteopontin, it reduced exogenous osteopontin levels.

Conclusions: COS selectively suppresses malignant phenotype by reducing fibronectin, and attenuates osteopontin expression and its functional contribution to migration in melanoma. This suggests that COS may serve as an adjuvant or preventive strategy to restrain melanoma progression and metastatic dissemination.

Keywords: chitosan oligosaccharide; melanoma; osteopontin; fibronectin; malignant phenotype

Introduction

Skin cancer is one of the most common malignancies worldwide, and despite extensive preventive efforts, its incidence continues to rise [1]. Melanoma, also known as cutaneous malignant melanoma, arises from dysregulated, abnormally proliferating melanocytes [2]. Germline or somatic mutations in genes and chronic exposure to ultraviolet radiation are well-established contributors to melanoma development [3]. Melanoma accounts for only a minority of skin cancers, but is responsible for most skin cancer–related deaths [4], emphasizing the need for continued mechanistic and translational research.

The biological activities of chitosan oligosaccharide (COS) and its related derivatives have received extensive research interest. The biological effects of COS on skin, including anti-tumor activity and its utility as a drug delivery carrier, vary according to molecular weight (or degree of polymerization), degree of deacetylation, and net charge. Nevertheless, these activities fundamentally relate to the structurally uniform backbone of COS, which is composed of repeating, positively charged d-glucosamine units [5]. Research since the late 2010s has increasingly emphasized chemistry and polymer science, whereas oncology-focused biological studies remain relatively scarce [6]. However, the combination of positive charge and immunomodulatory activity has made COS an attractive candidate for anticancer strategies [7]. Work that specifically focuses on skin cancer—and melanoma in particular—remains limited. Although it is known that low-molecular-weight chitosan may be more effective than high-molecular-weight forms, the specific contribution of COS has not been rigorously examined. While the antioxidant activity of COS (<1 kDa) has been reported in the murine melanoma cell line B16F10

[8], additional studies in melanoma have not been actively pursued.

Despite the reports mentioned above, mechanistic studies that systematically characterize the biological effects of COS in malignant melanoma are still lacking. Herein, we sought to delineate the actions of COS in melanoma progression. Because malignant behavior in melanoma is closely linked to cell motility, invasion, and metastatic potential, we focused on these phenotypes. The spheroid formation assay that evaluates growth under anoikis-resistant conditions is widely used to assess epithelial–mesenchymal transition (EMT)–related properties. Notably, the presence or absence of fetal bovine serum (FBS) or defined growth factors (GF) can modulate spheroid formation efficiency [9]. Therefore, we investigated whether COS could modulate malignant phenotypes in A2058 human melanoma cells, including spheroid formation and EMT or aggressiveness-associated marker expression, and evaluated COS as a candidate to suppress malignant progression.

Methods

COS Preparation

Dr. Jung Woo Kim kindly provided the lyophilized water-soluble COS (not-for-sale, KeyAllBio; Namwon, Jeonbuk, Republic of Korea). Immediately preceding each experiment, lyophilized COS was dissolved in distilled water, as previously described [5,10].

Cell Culture (2 Dimensional (D) Monolayer Culture)

A2058 human melanoma cell line, which have been authenticated by short tandem repeat (STR) profiling, was purchased from ATCC (Catalog No. CRL-3601; Manassas, VA, USA) and cultured in Dulbecco's modified Eagle's medium (DMEM; Catalog No. 10-013-CV, Corning Inc., Corning, NY, USA) supplemented with 10% FBS (Catalog No. 35-015-CV, Corning Inc.) and 1% penicillin/streptomycin (Catalog No. 30-002-CI, Corning Inc.) in a humidified incubator at 37 °C with 5% CO_2. Cell lines were routinely tested as negative for mycoplasma contamination using Myco-Visible mycoplasma rapid test kit (Catalog No. 3050901; MP Biomedicals, Solon, OH, USA), according to the manufacturer's instructions.

Cell Viability Assay

Cells were seeded in 96-well plates at a density of 2×10^3 cells per well. After overnight attachment, cells were treated first with increasing concentrations of COS (0, 31.25, 62.5, 125, 250, and 500 µg/mL). After 3 days (d), cell viability was assessed by 3-(4,5-dimethylthiazol-2-yl)-2,5-diphenyltetrazolium bromide (MTT) assay. Briefly, 20 µL of MTT solution (Catalog No. M6494, Thermo Fisher Scientific, Waltham, MA, USA; 5 mg/mL in phosphate buffered saline) was added to each well and incubated for an additional 3 h. Formazan crystals were solubilized, and absorbance at 595 nm with 620 nm as background was measured by VERSAmax microplate reader (Molecular Devices Korea LLC, Seoul, Republic of Korea). Viability was expressed as fold-change of the absorbance in vehicle-treated control wells (COS 0 µg/mL = 1).

Cells were then seeded, and treated with recombinant human osteopontin (OPN; Catalog No. ab281819, Abcam, Cambridge, MA, USA; 0, 1, 10, 100, and 1000 pg/mL) with or without COS (50 µg/mL). Cell viability was assessed by MTT assay, and expressed as previously described.

Wound Healing Assay

Cell migration was evaluated using a scratch assay as previously described [11]. In brief, three reference lines were drawn on the back of each well of a 6-well plate. A2058 cells were seeded at 2×10^5 cells per well and grown to >90% confluence, followed by serum starvation overnight. A linear scratch wound was made perpendicular to the reference lines using a 20 µL pipette tip. Cells were then treated with COS (0, 1, 10, 50, 100, and 250 µg/mL) in complete growth medium. Images were captured at baseline (0 h) and after 24 h using a BX-50 microscope equipped with DP70 camera (Olympus, Tokyo, Japan). Wound areas were quantified using ImageJ software (version 1.38 with the MRI wound healing tool, http://imagej.net/ij/). Migration was expressed as: wound area (fold) = wound area at 24 h / wound area at 0 h.

Cells were seeded and cultured to confluence as described above, then treated with OPN (0, 10, 100, 500, and 1000 pg/mL) in the absence or presence of COS (0 or 50 µg/mL) in complete growth medium. Wound closure was quantified as previously described.

Spheroid Formation Assay (3D Culture)

For round-bottom ultra-low attachment plates (Catalog No. 7007, Corning Inc.), 2×10^2 cells were cultured either in standard 2D culture medium (sphere/FBS group) or in DMEM/F12 (Catalog No. 10-090-CV, Corning Inc.) supplemented with 1% B27 (Catalog No. 17504-044, Thermo Fisher Scientific), 20 ng/mL epidermal growth factor (EGF; Catalog No. PHG0311, Gibco, Thermo Fisher Scientific), and 20 ng/mL basic fibroblast growth factor (Catalog No. 13256029; Gibco, Thermo Fisher Scientific; sphere/GF group) [9]. COS (0, 62.5, 125, and 250 µg/mL) was added at the indicated concentrations, and cultures were maintained for 7 d.

For flat-bottom ultra-low attachment plates (Catalog No. 3474, Corning Inc), cells were seeded at 2×10^3 cells per well in the 3D/FBS group and 5×10^3 cells per well in the 3D/GF group with COS (0, 1, 10, and 50 µg/mL), then maintained for 7 d. In addition, cells were seeded at 5×10^3 cells per well in the 3D/GF group with OPN (0, 1, 10, 100, and 1000 pg/mL), and with cultures maintained for 7 d.

Table 1. Primary antibodies used for Western Blot analysis.

Name (Catalog No.)	Company	Dilution
N-cadherin (4061)	Cell Signaling Tech (Beverley, MA, USA)	1:1000
S100β (ab52642)	Abcam (Cambridge, MA, USA)	1:2000
E-cadherin (sc-7870)	Santa Cruz Biotechnology (Santa Cruz, CA, USA)	1:2500
Fibronectin (sc-8422)		1:1000
GAPDH (sc-47724)		1:1000
SNAI1 (sc-271977)		1:2000
Vimentin (sc-6260)		1:5000
Alpha-smooth muscle actin (A5228)	Sigma-Aldrich (St. Louis, MO, USA)	1:2500
Osteopontin (22952-1-AP)	Proteintech (Rosemont, IL, USA)	1:2000

Spheroid images were captured by BX-50 microscope (Olympus; as previously described). Quantification was performed using iSolution Lite software (for Windows 10; IMT Inc., Irvine, CA, USA). Spheroids trapped by cell strainers (70 µm pore; Catalog No. 352350; Corning) were used in subsequent experiments [9,12].

Western Blot Analysis

A2058 cells were cultured under 2D conditions for 3 d or under 3D conditions for 7 d in the presence of COS (0, 1, 10, or 50 µg/mL). Cells and spheroids were lysed using T-PER™ protein extraction reagent (Catalog No. 78501, Thermo Fisher Scientific) containing 1% protease inhibitor cocktail (Catalog No. ab201111, Abcam), 0.5% phosphatase inhibitor cocktail I (Catalog No. ab201112, Abcam), and 0.5% phosphatase inhibitor cocktail II (Catalog No. ab201113, Abcam), followed by centrifugation at 13,300 rpm for 20 min to remove debris. Protein concentrations were determined by BCA assay kit (Catalog No. 23225, Thermo Fisher Scientific), according to the manufacturer's instructions.

Proteins (30 µg per lane) were separated by SDS-PAGE and transferred to polyvinylidene difluoride membranes (Catalog No. 162-0176, Bio-Rad, Hercules, CA, USA). Membranes were blocked with 5% skim milk (Catalog No. 232100; BD, Sparks, MD, USA) at room temperature (RT) for 1 h, then incubated overnight at 4 °C with primary antibodies (Table 1). After washing, membranes were incubated with appropriate secondary antibodies (Catalog No. PI-2000 and Catalog No. PI-1000, Vector Laboratories, Burlingame, CA, USA) for 1 h at RT. GAPDH was used as loading controls for cells and spheroids. Bands were visualized using enhanced chemiluminescence on an Azure™ c300 system (Azure Biosystems Inc., Dublin, CA, USA) and quantified with AzureSpot analysis software (version 14.2) [10].

Supernatants were collected under 2D conditions for 3 d or under 3D conditions for 7 d, in the presence of COS (0, 1, 10, or 50 µg/mL). In addition, conditioned media were collected from 2D and 3D/GF cultures supplemented with exogenous recombinant OPN (0, 1, 10, 100, and 1000 pg/mL) with or without COS (0 or 50 µg/mL). Supernatants were prepared as described above, and membranes stained with Ponceau S solution (Catalog No. BP076a; BIOSOLUTION, Suwon, Gyeonggi-do, Republic of Korea) according to the manufacturer's instructions. Routine immunoblotting for OPN was subsequently performed. Ponceau S staining of the Western blot was used as the loading control for supernatants. Recombinant human OPN itself was also used to confirm the molecular weight of the supernatants.

Immunohistochemistry

Human skin cancer tissue microarrays (Catalog No. CX2 human skin cancer–normal, and Catalog No. CK2 human malignant melanoma) were purchased from SuperBioChips Laboratories (Seoul, Republic of Korea). This study was granted exemption from ethical review by the Jeju National University Institutional Review Board (Approval No. JJNU-IRB-2025-081), and adhered to the principles of the Declaration of Helsinki. The arrays included normal skin (n = 9), melanoma (n = 59), and non-melanoma skin cancers (n = 40; 5 cores lost). Tumor were further stratified into early-stage (Stages I–II; melanoma n = 45, non-melanoma n = 21) and advanced-stage (Stage III–IV; melanoma n = 14, non-melanoma n = 14).

Sections were blocked with 10% normal horse serum (Catalog No. MP-7401, Vector Laboratories) for 1 h at RT, followed by overnight incubation at 4 °C with anti-OPN antibody (Catalog No. 22952-1-AP; Proteintech, Rosemont, IL, USA; diluted 1:100). After washing, sections were incubated with secondary antibodies (Catalog No. MP-7401, Vector Laboratories) for 1 h at RT, developed with diaminobenzidine, and counterstained with hematoxylin (Catalog No. H-3404; Vector Laboratories). Images were captured by BX-51 microscope with DP22 camera (Olympus). Staining intensity was scored negative (0), weak (1+), moderate (2+), or strong (3+).

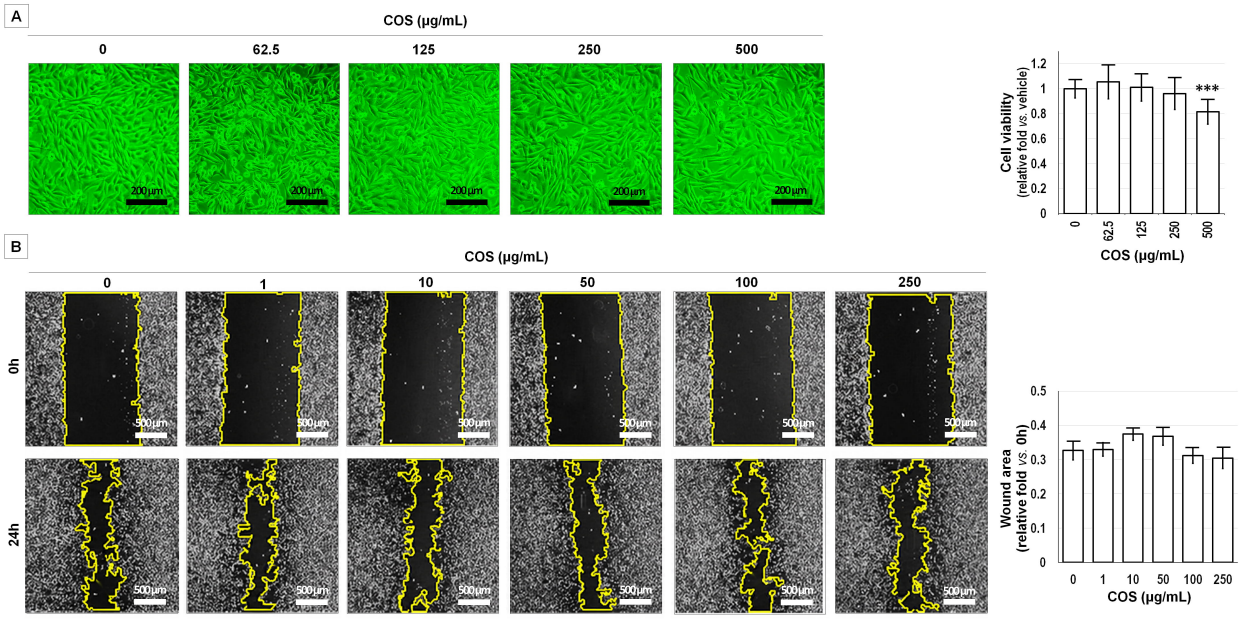

Fig. 1. Effects of chitosan oligosaccharides (COS) on melanoma cell viability and wound healing. (A) A2058 melanoma cells were treated with vehicle (distilled water, DW) or the indicated concentrations of COS for 3 d. Representative images are shown. Cell viability was assessed by MTT assay (n = 13). Data (fold changes) are shown as the mean ± SD. $^{***}p < 0.001$ vs. COS 0 μg/mL. (B) Changes in wound area following treatment with DW or the indicated concentrations of COS were measured (n = 12), as indicated, with representative images. Data (fold changes) are presented as the mean ± SD. MTT, 3-(4,5-dimethylthiazol-2-yl)-2,5-diphenyltetrazolium bromide; SD, standard deviation.

Statistical Analysis

All experiments were independently repeated at least three times. Data are presented as the mean ± standard deviation (SD). Data was subjected to statistical analysis using International Business Machines Corporation (IBM) SPSS Statistics (version 30; IBM Corp., Armonk, NY, USA), employing the Shapiro–Wilk normality test to assess normal distribution. For normally distributed data, one-way analysis of variance (ANOVA) and the Bonferroni or Tukey HSD *post hoc* test was applied. For non-normally distributed data, the Kruskal–Wallis H-test and Bonferroni *post hoc* test were utilized. Statistical significance between two groups was determined by independent samples *t*-test. A p-value < 0.05 was considered statistically significant.

Results

Effects of COS on Melanoma Cell Viability and Wound Healing

COS reduced the viability of A2058 melanoma cells in a concentration-dependent manner. Viability did not change significantly up to 250 μg/mL COS (0.95 ± 0.12-fold), but decreased to 0.79 ± 0.10-fold at 500 μg/mL ($p <$ 0.001) as compared to COS 0 μg/mL (Fig. 1A).

In the wound-healing assay, COS at concentrations up to 250 μg/mL did not significantly affect migration, as reflected by the wound area ($p = 0.232$; Fig. 1B).

Effects of COS on the Spheroid Formation of Melanoma

Under round-bottom condition (Fig. 2A), spheroid size in the 3D/FBS group decreased with COS in a concentration-dependent manner, whereas spheroid formation in the 3D/GF group was too limited for meaningful comparison. In the absence of COS, spheroid diameters were 438.1 ± 25.7 μm in the 3D/FBS group and 308.7 ± 23.4 μm in the 3D/GF group, indicating significantly poorer spheroid formation under GF-supplemented conditions ($p <$ 0.001). Adequate spheroids (>100 μm in diameter) were not observed in the 3D/GF group, even at 62.5 μg/mL COS.

Spheroid formation was also evaluated using flat-bottom ultra-low attachment plates (Fig. 2B). In both FBS- and GF-supplemented conditions, COS increased the number of spheroids in a concentration-dependent manner, while mean spheroid size decreased.

Effects of COS on EMT-Related Markers and Malignant Behavior-Related Protein Expression in Melanoma

First, environmental factors were compared among 2D, 3D/FBS, and 3D/GF under vehicle-treated conditions (Fig. 3). Of the proteins examined, significant changes were observed in fibronectin, α-smooth muscle actin (αSMA), N-cadherin, S100β, and CD44. Fibronectin, N-cadherin, and CD44 were significantly up-regulated in spheroids regardless of supplementations as compared to

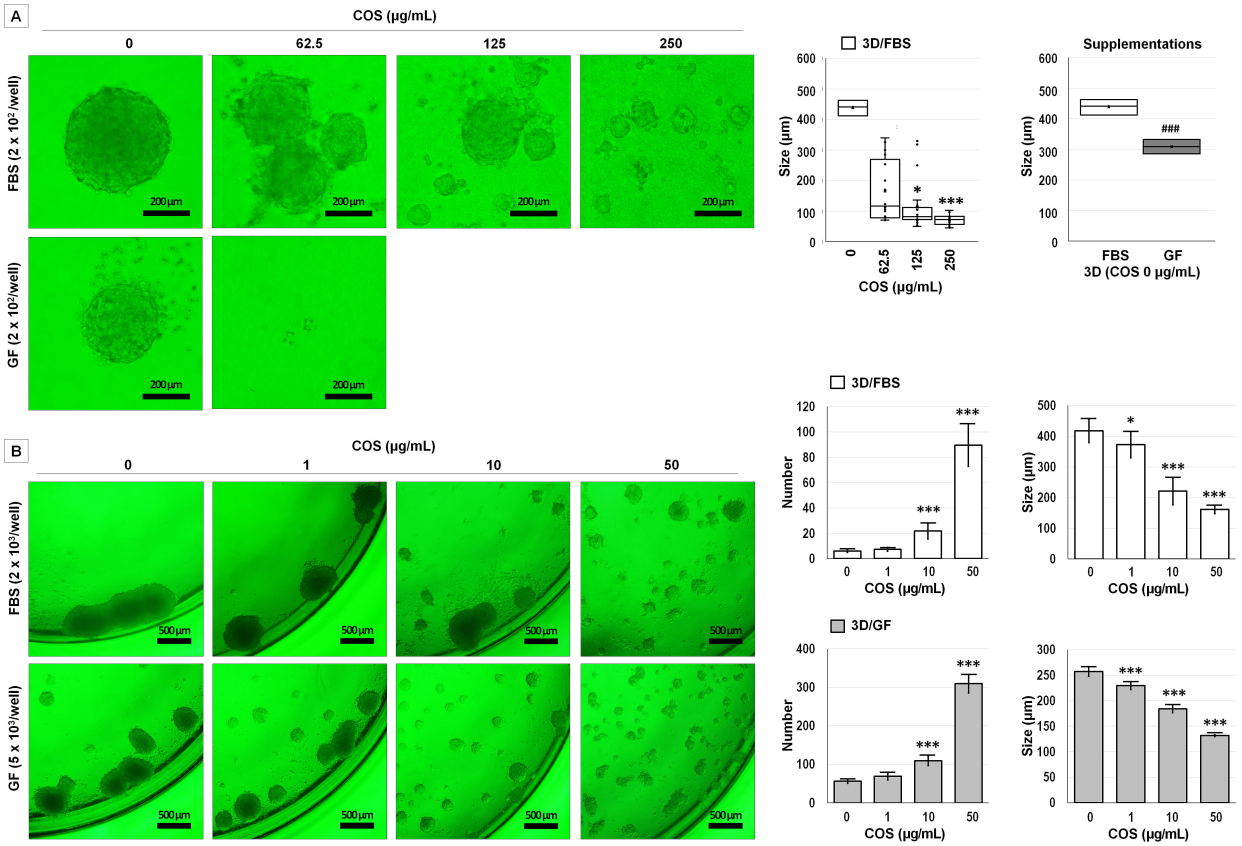

Fig. 2. Effects of chitosan oligosaccharides (COS) on the spheroid formation of melanoma. (A) Spheroid formation was induced in ultra-low attachment round-bottom wells under fetal bovine serum (FBS)- or growth factor (GF)-supplemented conditions. A2058 melanoma cells were treated with vehicle (distilled water, DW), or the indicated concentrations of COS, for 7 d. Representative images are shown. Spheroid sizes were measured (n = 3) and are expressed as the mean ± SD. $^{*}p < 0.05$, $^{***}p < 0.001$ vs. COS 0 μg/mL in 3D/FBS; $^{\#\#\#}p < 0.001$ vs. 3D/FBS. (B) Spheroid formation was performed in ultra-low attachment flat-bottom wells under FBS- or GF-supplemented conditions. Cells were treated for 7 d with DW, or the indicated concentrations of COS. Representative images are shown. Spheroid numbers and sizes were quantified (n = 12) and are presented as the mean ± SD. $^{*}p < 0.05$, $^{***}p < 0.001$ vs. COS 0 μg/mL.

2D cultured cells. αSMA and S100β showed differential responses between the 3D microenvironments, disclosing considerable increase only in the 3D/GF group.

Next, the dose-dependent effects of COS were examined in the 2D, 3D/FBS, and 3D/GF groups (Fig. 3A). Among all the proteins evaluated, fibronectin showed the most consistent and robust suppression by COS specifically in 3D cultures while exhibiting no significant effect in 2D monolayer culture. E-cadherin was significantly increased by COS in 2D and in 3D/FBS groups, but not in the 3D/GF group. The others showed no significant changes in all examined conditions.

In 2D or 3D/FBS conditions, OPN expression was not significantly altered by COS. However, in the 3D/GF cultures, COS at 50 μg/mL produced a significant reduction in OPN protein levels. In 2D culture, COS significantly increased CD44 expression. However, in 3D/FBS and 3D/GF conditions, this stimulatory effect was not observed (Fig. 3B).

Effects of COS on the OPN-Related Responses of Melanoma

To clarify the functional role of OPN, we treated cells with exogenous recombinant OPN (Fig. 4A). Exogenous OPN slightly but significantly increased the viability of A2058 melanoma cells, especially at 100 pg/mL OPN ($p = 0.048$). Under GF-supplemented conditions, exogenous OPN had no significant effect on spheroid formation (Fig. 4B). In the wound healing assay, OPN increased migration in a dose-dependent manner. The residual wound area decreased from 0.36 ± 0.03-fold in control to 0.16 ± 0.07-fold at 1000 pg/mL of OPN ($p < 0.001$) (Fig. 4C). However, in the presence of 50 μg/mL COS, the OPN-induced viability (Fig. 4D) and wound healing (Fig. 4E) were abolished.

OPN Immunostaining in Melanoma as a Marker of Malignancy

We compared OPN immunostaining in normal skin and tumor tissues using tissue microarrays (Fig. 5). The

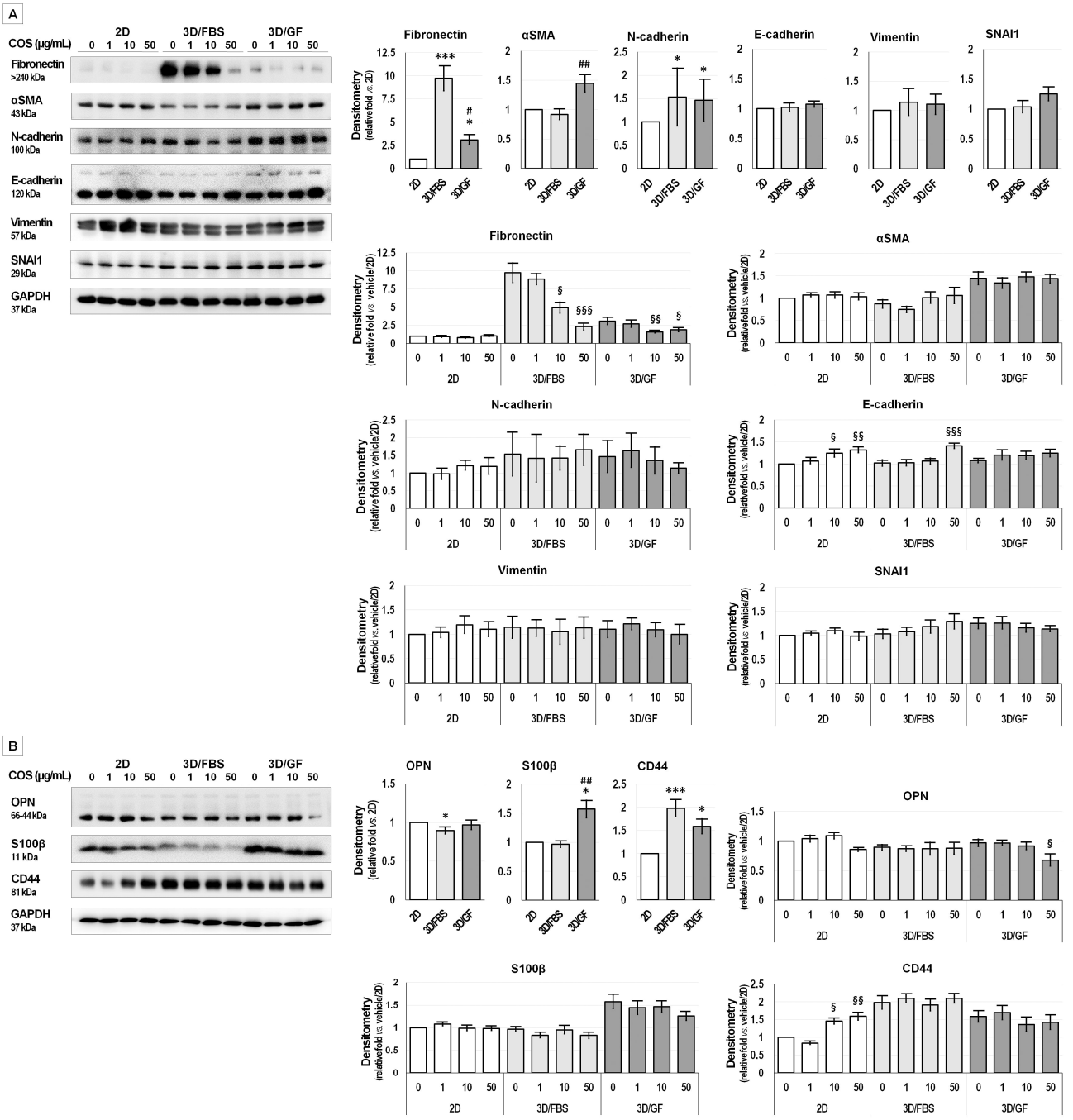

Fig. 3. Effects of chitosan oligosaccharides (COS) on the malignant behavior of melanoma. (A) A2058 cells were treated with distilled water (DW; COS 0 μg/mL) or the indicated concentrations of COS for 3 d in two-dimensional (2D) monolayer culture or in 3D spheroid culture for 7 d. Total protein extracts were subjected to immunoblotting for epithelial-mesenchymal transition-related proteins. GAPDH served as the loading control (n = 7). Band intensities were quantified using AzureSpot software. Data (fold-change) are represented as the mean ± SD. $^{*}p < 0.05$, $^{***}p < 0.001$ vs. COS 0 μg/mL in 2D; $^{\#}p < 0.05$, $^{\#\#}p < 0.01$ vs. 3D/FBS; $^{\S}p < 0.05$, $^{\S\S}p < 0.01$, $^{\S\S\S}p < 0.001$ vs. COS 0 μg/mL group within the same treatment condition. (B) Immunoblotting was performed for the aggressive markers of melanoma. GAPDH was used as the loading control. $^{*}p < 0.05$, $^{***}p < 0.001$ vs. COS 0 μg/mL in 2D; $^{\#\#}p < 0.01$ vs. 3D/FBS; $^{\S}p < 0.05$, $^{\S\S}p < 0.01$ vs. COS 0 μg/mL group within the same treatment condition.

mean ages were 64.8 ± 8.6 years for normal skin, 61.3 ± 12.9 years for non-melanoma, and 53.1 ± 15.3 years for melanoma, with melanoma patients being significantly younger ($p = 0.005$).

OPN immunoreactivity scores were higher in normal skin than in non-melanoma and melanoma. As compared with normal skin (2.67 ± 0.50), non-melanoma samples showed a significant decrease in Stages I–II (1.76 ± 0.70;

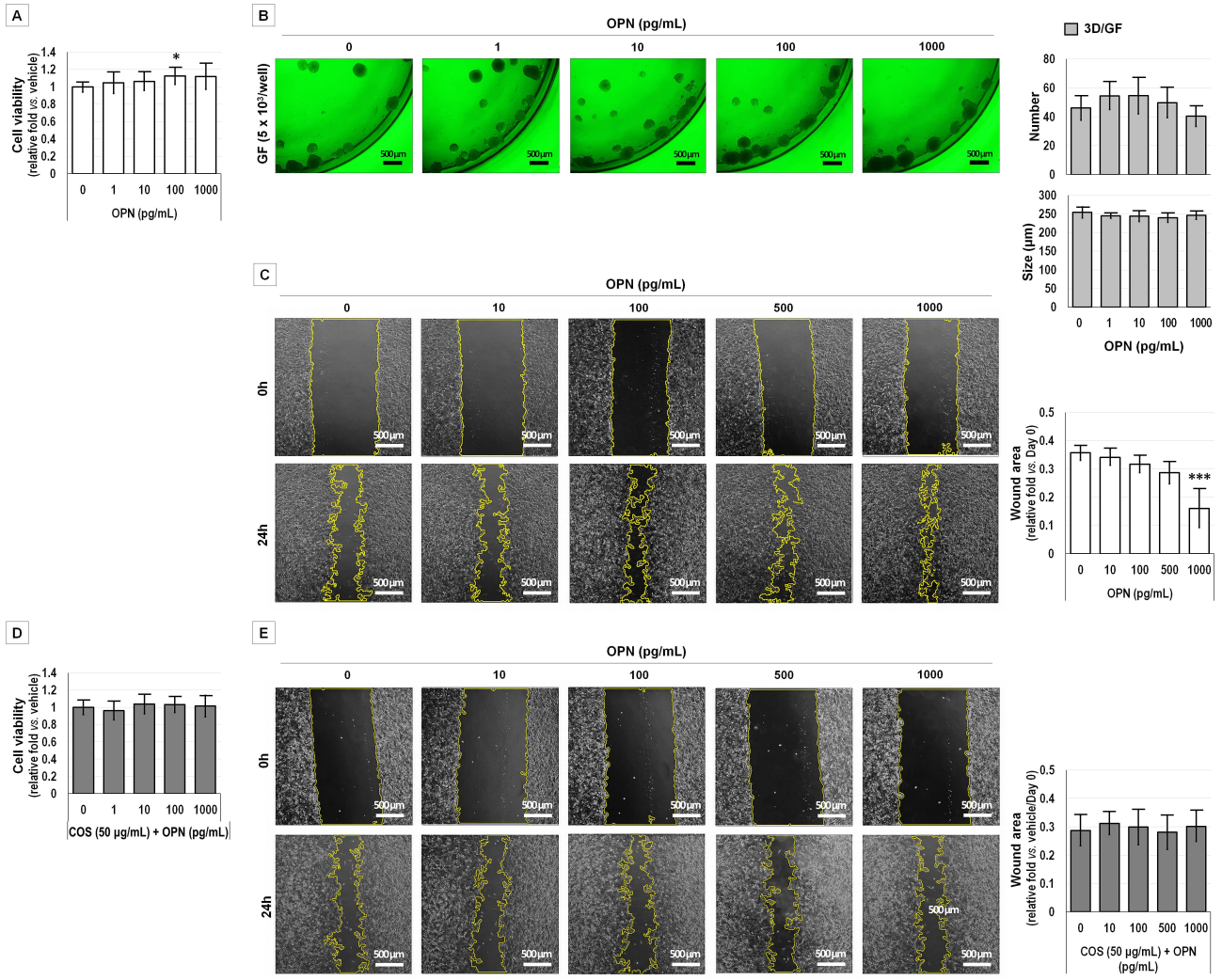

Fig. 4. Effects of exogenous osteopontin (OPN) with or without chitosan oligosaccharides (COS) on melanoma. (A) A2058 melanoma cells were treated with vehicle (distilled water, DW) or the indicated concentrations of exogenous OPN, for 3 d. Cell viability was assessed using the MTT assay (n = 12). Data (fold changes) are shown as the mean ± SD. $^{*}p < 0.05$ vs. OPN 0 pg/mL. (B) Spheroid formation was performed in ultra-low attachment flat-bottom wells under growth factor (GF)-supplemented conditions (3D/GF). Cells were treated with DW, or the indicated concentrations of OPN, for 7 d. Representative images are shown. Spheroid numbers and sizes were quantified (n = 10) and are presented as the mean ± SD. (C) Changes in wound area following treatment with DW or the indicated concentrations of OPN were measured (n = 6), as indicated, with representative images. Data (fold changes) are presented as the mean ± SD. $^{***}p < 0.001$ vs. OPN 0 pg/mL. (D) A2058 melanoma cells were treated with DW, or the indicated concentrations of exogenous OPN with 50 μg/mL of COS, for 3 d. Cell viability was assessed using the MTT assay (n = 12). Data (fold changes) are shown as the mean ± SD. (E) Changes in wound area following treatment with DW or the indicated concentrations of OPN with 50 μg/mL of COS were measured (n = 6), as indicated, with representative images. Data (fold changes) are presented as the mean ± SD.

$p = 0.002$) and in Stages III–IV (1.64 ± 0.63; $p = 0.002$). Melanoma showed a significant decrease only at Stages III–IV (2.00 ± 0.78; $p = 0.035$) compared to normal skin, but with considerable increase in Stages I–II (2.17 ± 0.79; $p = 0.034$) compared to Stages I–II in non-melanoma.

Effects of COS on the Secretory Fraction of OPN in Melanoma

Secretory OPN levels in conditioned media from the 2D, 3D/FBS, and 3D/GF groups under vehicle-treated conditions showed a significant decrease in 3D/GF, as compared with both 2D ($p < 0.001$) and 3D/FBS ($p < 0.001$). No dose-dependent changes with COS were observed in any condition (Fig. 6A).

Distinct results were observed in the 2D (Fig. 6B) and 3D/GF (Fig. 6C) cultures supplemented with exogenous OPN. In the presence of COS 50 μg/mL, exogenous OPN (1 ng/mL) was significantly decreased in the 2D ($p = 0.006$) and 3D/GF ($p < 0.001$) cultures.

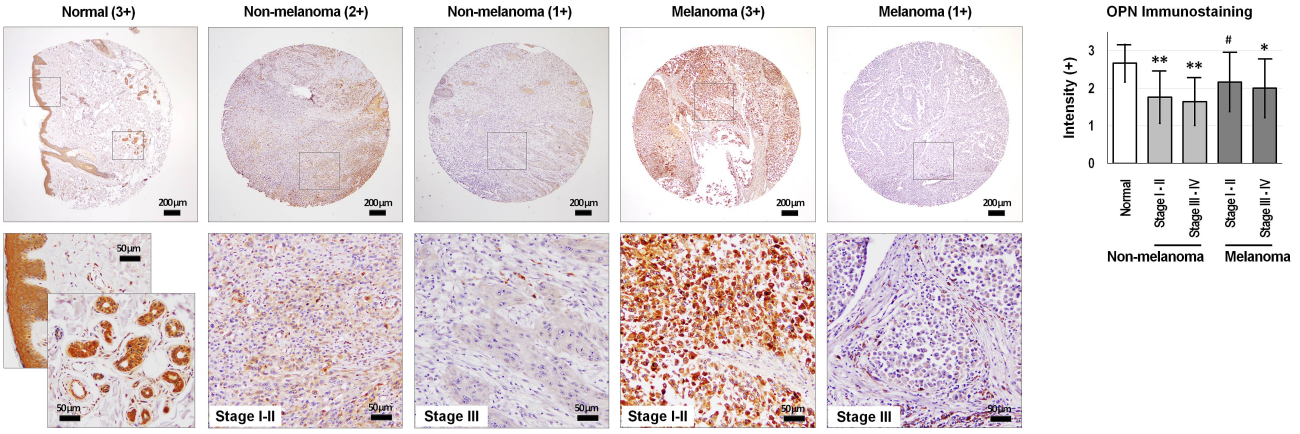

Fig. 5. Osteopontin (OPN) immunostaining in melanoma as a marker of malignancy. Tissue microarrays were immunostained with OPN antibody and their intensities scored. Data are presented as the mean ± SD. $^{*}p < 0.05$, $^{**}p < 0.01$ vs. normal; $^{\#}p < 0.05$, vs. Stages I–II of non-melanoma.

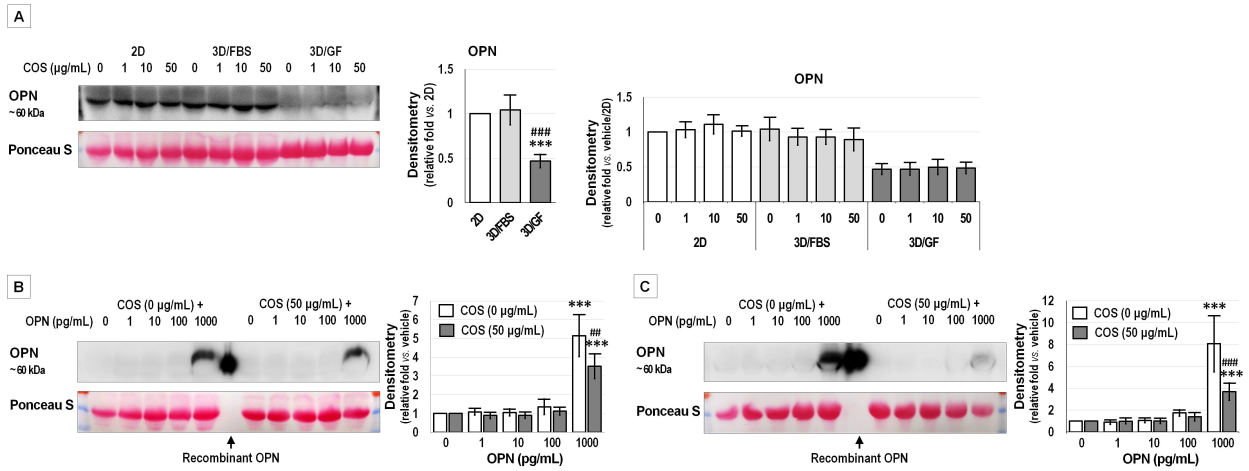

Fig. 6. Effects of chitosan oligosaccharides (COS) on the secretory fraction of osteopontin (OPN) and exogenous OPN in melanoma. (A) A2058 cells were treated with distilled water (DW; COS 0 μg/mL) or the indicated concentrations of COS for 3 d in two-dimensional (2D) monolayer culture, or for 7 d in 3D spheroid culture. Supernatants were collected and total protein extracts were subjected to immunoblotting for secretory OPN. Ponceau S staining served as the loading control (n = 7). Band intensities were quantified using AzureSpot software, and data (fold-change) are represented as the mean ± SD. $^{***}p < 0.001$ vs. 2D; $^{\#\#\#}p < 0.01$ vs. 3D/FBS. (B) Exogenous recombinant OPN was added in the 2D cultures for 3 d, with or without COS (50 μg/mL). Supernatants were used to detect exogenous OPN, as previously described (n = 7). Ponceau S staining of the Western blot was used as the loading control. The arrow indicates recombinant OPN protein to confirm the molecular weight. Data (fold-change) are represented as the mean ± SD. $^{***}p < 0.001$ vs. OPN 0 pg/mL; $^{\#\#}p < 0.01$ vs. COS 0 μg/mL. (C) Exogenous recombinant OPN was added in the 3D cultures supplemented with growth factors for 7 d, with or without COS (50 μg/mL). Supernatants were used to detect exogenous OPN, as previously described (n = 7). The arrow indicates recombinant OPN protein. Data (fold-change) are represented as the mean ± SD. $^{***}p < 0.001$ vs. OPN 0 pg/mL; $^{\#\#\#}p < 0.001$ vs. COS 0 μg/mL.

Discussion

Although the 50% cytotoxicity concentration (CC_{50}) of COS in colorectal cancer cell lines has been reported to be approximately 500 μg/mL [10], A2058 melanoma cells are relatively less sensitive to COS in terms of viability. Notably, spheroid formation was inhibited at substantially lower concentrations (50 μg/mL), suggesting COS may preferentially affect 3D malignant phenotypes rather than exerting direct cytotoxicity.

Consistent with previous findings [9], fibronectin levels increased in the spheroid cultures as compared to 2D culture, while the 3D/GF group showed decreased expression in fibronectin and increased expression in αSMA as compared to the 3D/FBS group. While robust changes in E-cadherin-related biology have been reported using

spheroid formation [9,12], in our melanoma model, E-cadherin did not show a strong association with spheroid formation. S100β and OPN are among the most widely used serum markers linked to melanoma aggressiveness [13]. In the present study, S100β increased significantly under the sphere/GF group but was not altered by COS in a dose-dependent manner. In contrast, OPN was reduced by COS in 2D and under the sphere/GF groups. While exogenous recombinant OPN enhanced migration in a dose-dependent manner, low-dose COS (50 μg/mL) abolished this effect. Although secretory fraction of OPN was not changed under COS treatment, exogenous OPN was significantly decreased in the presence of COS. COS with positive charges could interact with proteins [14,15], which interaction is related to the molecular weight, deacetylation degree, etc. [16,17]. Thus, COS has been proposed as a protein-binding material [17], with lower molecular weight forming more stable COS-protein complexes. Collectively, these observations support a functional role for OPN in melanoma cell migration and demonstrate that low-dose COS can suppress OPN-driven migration via suppressing its expression or binding to the secretory fraction of OPN. While anti-cancer effects of COS have been reported [18,19], to the best of our knowledge, comparable functional data in melanoma have been limited.

The interplay between OPN and fibronectin has been recognized for decades [20], and is consistent with our findings. Downregulation of E-cadherin and upregulation of OPN have been implicated in the enhanced invasive potential of melanoma [21]. In our study, OPN, rather than S100β, appeared to play a central role in migratory behavior, and COS attenuated OPN expression and its functional contribution to migration, highlighting a potential mechanism for anti-metastatic activity. Notably, COS has been reported to modulate OPN levels suppressed by dexamethasone in an osteoporosis model [22], an effect in the opposite direction to our findings. Nevertheless, COS may have utility in CD44 overexpressing triple-negative breast cancers [23]. In addition, secreted fraction of OPN can suppress the $CD8^+$ T cells through CD44 engagement in uveal melanoma, suggesting an OPN-CD44 axis [24]. In this study, COS did not affect CD44 expression in 3D culture conditions, while OPN was decreased in the 3D/GF group.

The relationship between COS and GF signaling is also noteworthy. COS inhibits EGF receptor (EGFR) and mitogen-activated protein kinases signaling, thereby suppressing EGF-induced proliferation and EMT-like morphological changes [25]. In melanoma, siRNA-mediated knockdown of OPN has been shown to inhibit proliferation and invasion via EGFR-dependent mechanisms [26]. These observations suggest that a COS–OPN–EGFR axis may be particularly relevant in GF-rich microenvironments. Future studies using melanoma cell lines with more robust spheroid formation under GF conditions will help dissect these interactions in more detail.

Immunohistochemical analyses of tumor tissues have yielded inconsistent results. Melanoma often shows stronger OPN staining than benign nevi, however, the relationship between OPN expression and metastatic status is less clear [27]. A recent report suggested that circulating OPN may promote primary tumor growth without necessarily correlating with spontaneous metastasis [28]. In addition, specific OPN isoforms, OPNc, have been linked to invasive behavior [29]. In our tissue microarray analysis, OPN staining was higher in normal skin than in melanoma and decreased further with stage advancement. These discrepancies underscore the importance of careful antibody selection, isoform considerations, and validation strategies in melanoma immunohistochemistry.

Because melanoma disseminates via lymphatic and hematogenous routes [30,31], factors influencing tumor-vascular interactions are particularly relevant. OPN has been implicated both in EMT, and as a lymphangiogenic factor that can promote metastatic spread [32]. COS has also been reported to exert anti-angiogenic activity [33]. Moreover, partially acetylated COS inhibited the adhesion of hepatocellular carcinoma cells to vascular endothelium, with low concentration effectively suppressing vascular invasion [18]. These observations support the possibility that non-cytotoxic COS concentrations may still produce meaningful anti-metastatic effects by modulating the tumor–vascular interface. In this context, the positively charged nature of COS warrants further investigation in cancer research [34]. Redox/pH-responsive COS derivatives have been developed to overcome multidrug resistance [35], and COS has demonstrated synergistic anti-tumor effects with other chemotherapeutic agents in a melanoma model [36]. Our previous results [10] have also shown that COS can enhance the anti-cancer effects of 5-fluorouracil in colorectal cancers.

This study has limitations. First, our experiments were performed using only one melanoma cell line; additional cell lines are needed to generalize the findings. Second, prior studies have evaluated OPN-driven invasion at higher concentrations (e.g., 5 μg/mL) [37]. Here, we tested OPN up to 1 ng/mL, and cannot exclude potential effects at higher doses. Although serum OPN levels up to 87.3 ng/mL have been reported in metastatic melanoma [13], *in vitro* conditions may not fully recapitulate the *in vivo* conditions. Third, although exogenous OPN decreased under COS treatment, the concentration of secretory fraction of OPN in culture supernatants might be too low to detect via Western Blotting. Therefore, more sensitive methods to detect low concentration of OPN or molecular docking between COS and OPN would support these findings. Fourth, the relationship between EMT and stemness was not fully examined, although CD44 is considered as an EMT and stem cell marker [38]. Finally, although we provided tissue microarray data, further validation in animal models and/or liquid biopsy specimens would strengthen translational rel-

evance and enable direct comparisons between tissues and circulating OPN levels.

Conclusions

This study demonstrates that at relatively low, non-cytotoxic concentrations, COS selectively suppresses malignant phenotypes by reducing fibronectin and attenuates OPN expression or its secretory fraction and its functional contribution to migration in A2058 melanoma cells. This finding suggests that COS may have potential as an adjuvant or preventive strategy to restrain melanoma progression and metastatic dissemination, and warrants further preclinical and translational investigation.

Abbreviations

COS, Chitosan oligosaccharide; EMT, Epithelial-mesenchymal transition; FBS, Fetal bovine serum; GF, Growth factor; D, Dimensional; OPN, Osteopontin; DMEM, Dulbecco's modified Eagle's medium; EGF, Epidermal growth factor; EGFR, EGF receptor; SD, Standard deviation; ANOVA, Analysis of variance; CC_{50}, 50% cytotoxicity concentration.

Availability of Data and Materials

The datasets generated or analyzed during the current study are available from the corresponding author upon reasonable request.

Author Contributions

Study conception and design: SPY; Data collection: IYC, HJB, and JWH; Analysis and interpretation of results: IYC and YHM; Draft manuscript preparation: IYC and SPY. All authors have been involved in revising it critically for important intellectual content. All authors gave final approval of the version to be published. All authors have participated sufficiently in the work to take public responsibility for appropriate portions of the content and agreed to be accountable for all aspects of the work in ensuring that questions related to its accuracy or integrity.

Ethics Approval and Consent to Participate

The study was approved by the Institutional Review Board of Jeju National University (JJNU-IRB-2025-081), and adhered to the principles of the Declaration of Helsinki. As the tissue microarrays were commercially obtained and fully de-identified, the requirement for informed consent was waived by the Institutional Review Board.

Acknowledgment

Not applicable.

Funding

This research was supported by the Basic Science Research Program through the National Research Foundation of Korea (NRF) funded by the Ministry of Education (RS-2023-00270936).

Conflict of Interest

The authors declare no conflict of interest.

References

[1] Andreikos DA, Spandidos DA. Telomere length and skin cancer risk: A systematic review and meta-analysis of melanoma, basal cell carcinoma and squamous cell carcinoma. Oncology Letters. 2025; 30: 395. https://doi.org/10.3892/ol.2025.15141

[2] Wagstaff W, Mwamba RN, Grullon K, Armstrong M, Zhao P, Hendren-Santiago B, et al. Melanoma: Molecular genetics, metastasis, targeted therapies, immunotherapies, and therapeutic resistance. Genes & Diseases. 2022; 9: 1608–1623. https://doi.org/10.1016/j.gendis.2022.04.004

[3] Conforti C, Zalaudek I. Epidemiology and Risk Factors of Melanoma: A Review. Dermatology Practical & Conceptual. 2021; 11: e2021161S. https://doi.org/10.5826/dpc.11S1a161S

[4] Davey MG, Miller N, McInerney NM. A Review of Epidemiology and Cancer Biology of Malignant Melanoma. Cureus. 2021; 13: e15087. https://doi.org/10.7759/cureus.15087

[5] Lee SH, Kim JW, Hyun JW, Kim HJ, Yoon SP. Biological effects of chitosan oligosaccharides on the skin and their clinical applicability. Carbohydrate Research. 2025; 555: 109588. https://doi.org/10.1016/j.carres.2025.109588

[6] Yuan X, Zheng J, Jiao S, Cheng G, Feng C, Du Y, et al. A review on the preparation of chitosan oligosaccharides and application to human health, animal husbandry and agricultural production. Carbohydrate Polymers. 2019; 220: 60–70. https://doi.org/10.1016/j.carbpol.2019.05.050

[7] Zhai X, Li C, Ren D, Wang J, Ma C, Abd El-Aty AM. The impact of chitooligosaccharides and their derivatives on the in vitro and in vivo antitumor activity: A comprehensive review. Carbohydrate Polymers. 2021; 266: 118132. https://doi.org/10.1016/j.carbpol.2021.118132

[8] Mendis E, Kim MM, Rajapakse N, Kim SK. An in vitro cellular analysis of the radical scavenging efficacy of chitooligosaccharides. Life Sciences. 2007; 80: 2118–2127. https://doi.org/10.1016/j.lfs.2007.03.016

[9] Chang IY, Yoon SP. Increased soluble E-cadherin of spheroid formation supplemented with fetal bovine serum in colorectal cancer cells. Oncology Letters. 2023; 25: 207. https://doi.org/10.3892/ol.2023.13793

[10] Han JS, Boo HJ, Hyun JW, Song H, Chang IY, Yoon SP. Chitosan oligosaccharide enhances the anti-cancer effects of 5-fluorouracil on SNU-C5 colorectal cancer cells by activating ERK. Oncology Research. 2025; 33: 873–884. https://doi.org/10.32604/or.2024.052003

[11] Yoon C, Na E, Choi MJ, Yoon SP. Upregulation of Sox2 Following Saracatinib Treatment Contributes to a Resistant Phenotype in Colorectal Cancer Cells under Growth Factor-Supplemented Conditions. Oncology Research. 2026; 34: 23. https://doi.org/10.32604/or.2026.074140

[12] Chang IY, Boo HJ, Hyun JW, Yoon SP. The feasible role of soluble E-cadherin in spheroidogenesis of HCT116 colorectal cancer cells, a candidate biomarker for liquid biopsy. Oncology Letters. 2025; 29: 245. https://doi.org/10.3892/ol.2025.14991

[13] Várvölgyi T, Janka EA, Szász I, Koroknai V, Toka-Farkas T, Szabó IL, et al. Combining Biomarkers for the Diagnosis of Metastatic Melanoma. Journal of Clinical Medicine. 2023; 13: 174. https://doi.org/10.3390/jcm13010174

[14] Wang L, Wang L, Wang N, Song C, Wen C, Yan C, et al. Fucoidan alleviates the inhibition of protein digestion by chitosan and its oligosaccharides. International Journal of Biological Macromolecules. 2024; 269: 132072. https://doi.org/10.1016/j.ijbiomac.2024.132072

[15] Zhao X, Yang C, Liu W, Lu K, Yin H. Inhibition of insulin fibrillation by carboxyphenylboronic acid-modified chitosan oligosaccharide based on electrostatic interactions and hydrophobic interactions. Biophysical Chemistry. 2024; 310: 107236. https://doi.org/10.1016/j.bpc.2024.107236

[16] Roman DL, Ostafe V, Isvoran A. Computational Assessment of Chito-Oligosaccharides Interactions with Plasma Proteins. Marine Drugs. 2021; 19: 120. https://doi.org/10.3390/md19030120

[17] Li J, Guan S, Cai B, Li Q, Rong S. Low molecular weight chitosan oligosaccharides form stable complexes with human lactoferrin. FEBS Open Bio. 2023; 13: 2215–2223. https://doi.org/10.1002/2211-5463.13722

[18] Jing B, Cheng G, Li J, Wang ZA, Du Y. Inhibition of Liver Tumor Cell Metastasis by Partially Acetylated Chitosan Oligosaccharide on A Tumor-Vessel Microsystem. Marine Drugs. 2019; 17: 415. https://doi.org/10.3390/md17070415

[19] Liu H, Ding S, Lyu W, Lu S, Liu X. Chito-oligosaccharide impairs the proliferation, invasion and migration of pancreatic cancer cells. Discover Oncology. 2025; 16: 298. https://doi.org/10.1007/s12672-025-02015-2

[20] Mukherjee BB, Nemir M, Beninati S, Cordella-Miele E, Singh K, Chackalaparampil I, et al. Interaction of osteopontin with fibronectin and other extracellular matrix molecules. Annals of the New York Academy of Sciences. 1995; 760: 201–212. https://doi.org/10.1111/j.1749-6632.1995.tb44631.x

[21] Smit DJ, Gardiner BB, Sturm RA. Osteonectin downregulates E-cadherin, induces osteopontin and focal adhesion kinase activity stimulating an invasive melanoma phenotype. International Journal of Cancer. 2007; 121: 2653–2660. https://doi.org/10.1002/ijc.23039

[22] Vimalraj S, Govindarajan D, Sudhakar S, Suresh R, Palanivel P, Sekaran S. Chitosan derived chito-oligosaccharides promote osteoblast differentiation and offer anti-osteoporotic potential: Molecular and morphological evidence from a zebrafish model. International Journal of Biological Macromolecules. 2024; 259: 129250. https://doi.org/10.1016/j.ijbiomac.2024.129250

[23] Ding Y, Yang R, Yu W, Hu C, Zhang Z, Liu D, et al. Chitosan oligosaccharide decorated liposomes combined with TH302 for photodynamic therapy in triple negative breast cancer. Journal of Nanobiotechnology. 2021; 19: 147. https://doi.org/10.1186/s12951-021-00891-8

[24] Ge T, Yang Y, Zhang W, Li M, Gu X, Yang L, et al. Tumor-intrinsic redox programming drives an SPP1-CD44 axis of immune suppression in uveal melanoma. Redox Biology. 2026; 90: 104011. https://doi.org/10.1016/j.redox.2026.104011

[25] Xu Q, Wang W, Yang W, Du Y, Song L. Chitosan oligosaccharide inhibits EGF-induced cell growth possibly through blockade of epidermal growth factor receptor/mitogen-activated protein kinase pathway. International Journal of Biological Macromolecules. 2017; 98: 502–505. https://doi.org/10.1016/j.ijbiomac.2017.02.021

[26] Kiss T, Jámbor K, Koroknai V, Szász I, Bárdos H, Mokánszki A, et al. Silencing Osteopontin Expression Inhibits Proliferation, Invasion and Induce Altered Protein Expression in Melanoma Cells. Pathology Oncology Research : POR. 2021; 27: 581395. https://doi.org/10.3389/pore.2021.581395

[27] Maier T, Laubender RP, Sturm RA, Klingenstein A, Korting HC, Ruzicka T, et al. Osteopontin expression in plasma of melanoma patients and in melanocytic tumours. Journal of the European Academy of Dermatology and Venereology : JEADV. 2012; 26: 1084–1091. https://doi.org/10.1111/j.1468-3083.2011.04210.x

[28] Saup R, Nair N, Shen J, Schmaus A, Thiele W, Garvalov BK, et al. Increased Circulating Osteopontin Levels Promote Primary Tumour Growth, but Do Not Induce Metastasis in Melanoma. Biomedicines. 2023; 11: 1038. https://doi.org/10.3390/biomedicines11041038

[29] Koroknai V, Szász I, Jámbor K, Balázs M. Expression pattern of osteopontin isoforms in malignant melanoma cell lines. Clinical and Translational Science. 2024; 17: e13694. https://doi.org/10.1111/cts.13694

[30] Naves LB, Dhand C, Venugopal JR, Rajamani L, Ramakrishna S, Almeida L. Nanotechnology for the treatment of melanoma skin cancer. Progress in Biomaterials. 2017; 6: 13–26. https://doi.org/10.1007/s40204-017-0064-z

[31] Liu J, Fukunaga-Kalabis M, Li L, Herlyn M. Developmental pathways activated in melanocytes and melanoma. Archives of Biochemistry and Biophysics. 2014; 563: 13–21. https://doi.org/10.1016/j.abb.2014.07.023

[32] Liersch R, Shin JW, Bayer M, Schwöppe C, Schliemann C, Berdel WE, et al. Analysis of a novel highly metastatic melanoma cell line identifies osteopontin as a new lymphangiogenic factor. International Journal of Oncology. 2012; 41: 1455–1463. https://doi.org/10.3892/ijo.2012.1548

[33] Huang X, Jiao Y, Zhou C. Impacts of chitosan oligosaccharide (COS) on angiogenic activities. Microvascular Research. 2021; 134: 104114. https://doi.org/10.1016/j.mvr.2020.104114

[34] Li B, Cui J, Xu T, Xu Y, Long M, Li J, et al. Advances in the preparation, characterization, and biological functions of chitosan oligosaccharide derivatives: A review. Carbohydrate Polymers. 2024; 332: 121914. https://doi.org/10.1016/j.carbpol.2024.121914

[35] Jia L, Li Z, Zheng D, Li Z, Zhao Z. A targeted and redox/pH-responsive chitosan oligosaccharide derivatives based nanohybrids for overcoming multidrug resistance of breast cancer cells. Carbohydrate Polymers. 2021; 251: 117008. https://doi.org/10.1016/j.carbpol.2020.117008

[36] Zhang X, Chen W, Zhang K, Liu Z, Lyu Q, Jin L, et al. Exploration of the Synergistic Effect of Chitosan Oligosaccharide and Dacarbazine (DTIC) in the Treatment of Melanoma. Current Cancer Drug Targets. 2026. https://doi.org/10.2174/0115680096423297251202110111 (online ahead of print)

[37] Hayashi C, Rittling S, Hayata T, Amagasa T, Denhardt D, Ezura Y, et al. Serum osteopontin, an enhancer of tumor metastasis to bone, promotes B16 melanoma cell migration. Journal of Cellular Biochemistry. 2007; 101: 979–986. https://doi.org/10.1002/jcb.21298

[38] Weitzenböck HP, Gschwendtner A, Wiesner C, Depke M, Schmidt F, Trautinger F, et al. Proteome analysis of NRF2 inhibition in melanoma reveals CD44 up-regulation and increased apoptosis resistance upon vemurafenib treatment. Cancer Medicine. 2022; 11: 956–967. https://doi.org/10.1002/cam4.4506